Effect of Control Surface Mass Unbalance on the Stability of a Closed-Loop Active Control System

E. Nissim

NASA

Effect of Control Surface Mass Unbalance on the Stability of a Closed-Loop Active Control System

E. Nissim
Ames Research Center
Dryden Flight Research Facility
Edwards, California

CONTENTS

ABSTRACT

The effects on stability of inertial forces arising from closed-loop activation of mass-unbalanced control surfaces are studied analytically using inertial energy approach, similar to the aerodynamic energy approach used for flutter suppression. The limitations of a single control surface like a leading-edge (L.E.) control or a trailing-edge (T.E.) control are demonstrated and compared to the more powerful combined L.E.–T.E. mass unbalanced system. It is shown that a spanwise section for sensor location can be determined which ensures minimum sensitivity to the mode shapes of the aircraft. It is shown that an L.E. control exhibits compatibility between inertial stabilization and aerodynamic stabilization, and that a T.E. control lacks such compatibility. The results of the present work should prove valuable, when flutter is suppressed using mass unbalanced control surfaces, or for the stabilization of structural modes of large space structures by means of inertial forces.

NOMENCLATURE

a_{ii}	scalar gains, see eq. (36)
$a(\omega)$	transfer function defined in eq. (45)
b	reference semichord length
b_{ij}	element i,j of the $[B_c]$ matrix
b_R	semichord length at the reference section
b_y	$= \frac{\partial b}{\partial y}$
c_{ij}	element i,j of the real part of $[T]$
d_{ij}	element i,j of the imaginary part of $[T]$
e_{ii}	scalar gains, see eqs. (36)
h	plunge coordinate, positive down
h_R	plunge coordinate at the reference section, positive down
$\bar{h}_R$	$= h_R/b_R$
h_y	$= \frac{\partial h}{\partial y}$
M	mass of the strip
M_L	mass of the L.E. control
M_T	mass of the T.E. control
$\bar{M}_L$	$= M_L/M$
$\bar{M}_T$	$= M_T/M$
n	number of structural modes
p_i	transfer function pole location
r	number of control
s	reference length, of the Laplace variable
$\bar{t}_{ii}$	$a_{ii} + ie_{ii}$
t_{ij}	defined in eq. (36)
y	spanwise coordinate, measured from the reference section
y_{GL}	spanwise distance of L.E. control surface center of gravity measured from reference section
y_{GT}	spanwise distance of T.E. control surface center of gravity measured from reference section
$\bar{y}_{GL}$	$= y_{GL}/b_r$
$\bar{y}_{GT}$	$= y_{GT}/b_r$
α	pitching angle, positive nose up
α_y	$= \frac{\partial \alpha}{\partial y}$
α_R	angle of attack at reference section of activated strip
$\bar{\alpha}_y$	$= \alpha_y/\alpha_R$
β	leading-edge control deflection, positive nose down.
δ	trailing-edge control deflection, positive trailing edge down
λ	eigenvalue
λ_1	largest eigenvalue of a binary system
λ_2	smallest eigenvalue of a binary system
ρ	fluid density
ω	frequency
ω_n	natural frequency

Matrix Notation

$[A_R]$, $[A_I]$	real and imaginary parts of aerodynamic matrix, respectively, (order $n \times (n + r)$)
$[A_{R,s}]$, $[A_{I,s}]$	real and imaginary parts, respectively, of the aerodynamic matrix associated with the structural modes (order $n \times n$)
$[A_{R,c}]$, $[A_{I,c}]$	real and imaginary parts, respectively, of the aerodynamic matrix that couples the control surfaces with the structural modes (order $n \times r$)
$[B]$.	mass matrix (order $n \times (n + r)$)
$[B_s]$	structural mass matrix (order $n \times n$)
$[B_c]$	coupling mass matrix, between structural modes and control surfaces (order $n \times r$)
$[E]$	stiffness matrix (order $n \times (n + r)$)
$[E_s]$	structural stiffness matrix (order $n \times n$)
$[E_c]$	coupling stiffness matrix, between structural modes and control surfaces (order $n \times r$)
$\{F\}$	column matrix of forces (order n)
$[Q_R]$, $[Q_I]$	real and imaginary parts, respectively, of the energy eigenvectors (of matrix $[Q]$ (order $n \times n$))
$\{q\}$	column of structural responses (order n)
$\{\bar{q}\}$	column of structural and control responses of order $(n + r)$, see eq. (3)
$\{q_0\}$	column of structural response amplitudes (order n)
$\{q_c\}$	column of control surface responses (order r)
$[T]$	matrix representing control law transfer functions (order $r \times n$)
$[U]$	energy eigenvalue matrix, see eq. (8) (order $n \times n$)

$\{\xi_R\}, \{\xi_I\}$	real and imaginary parts, respectively, of the energy principal coordinates, see eq. (12)

Superscripts

T	transposed matrix
*	conjugate

Subscripts

c	relates to control surfaces
s	relates to the main structure of the system
R	relates to the reference section within the 2-D strip

INTRODUCTION

Studies concerning flutter suppression using active controls concentrate on the numerical design of control laws and their effects on the resulting performance of the system (Mukhopadhyay and others 1981, Newsom 1979, Newsom and others 1980, Nissim and Abel 1978, Mahesh and others 1981, and Freymann 1987). In these studies, the system is considered to be fixed, and no attempt is made to investigate the possible effects of varying some of the aircraft parameters on the resulting control law and the overall system performance. Even for existing systems, there are some parameters that can be readily changed, like the mass balancing of control surfaces or the control surface actuator dynamics.

In the following, the effects of control surface mass unbalance of active control systems on the closed-loop stability of the systems are studied. This problem is relevant because aerodynamic control surfaces are naturally unbalanced. The balancing of these control surfaces requires the addition of non-negligible masses. Because an investment is made in an active control surface in terms of the mass of the elements required to drive the control surface, one is naturally tempted to avoid adding further masses to balance the active control surface. An analytic approach to the problem was adopted so that the results obtained would be informative regarding general systems rather than for a specific specialized system. For this reason, a two-dimensional model is considered, representing a

2

possible strip of a finite wing. To avoid assigning frequencies or mass values to this strip (since continuous wings have, effectively, an infinite number of frequencies, masses, and mode shapes), an energy approach was adopted, whereby the work done by the inertial mass–unbalanced forces per one cycle of oscillation was evaluated (Nissim 1971 and 1977). If these forces do a positive work on their surroundings, the system is dissipative. If, on the other hand, these forces do a negative work on their surroundings— implying that a positive work is done on the system—the system absorbs energy and is unstable. Hence, the sign of the work done by the unbalanced inertial forces indicates their potential contribution to either stability or to instability.

The major part of the work presented herein relates to a 2-D rigid strip performing pure pitch–plunge oscillations. In the final part of this work, the strip is allowed to twist along its span, to vary its chord length along the span, and to rotate as a result of the wing's bending oscillations. It is shown that this more realistic, generalized strip geometry and motion can be reduced for simple geometries and appropriate selection of reference section to yield results identical to the 2-D pitch–plunge rigid strip.

INERTIAL ENERGY APPROACH

Basic Equations

Let the n equations

$$\{F\} = -\omega^2 [B + \pi\rho b^4 s(A_R + iA_I)]\{\bar{q}\} + [E]\{\bar{q}\}$$
(1)

represent the generalized equations of motion of n structural modes with r-activated controls, where at flutter

$$\{F\} = 0$$

and

ω	frequency
[B]	mass matrix
$[A_R]$, $[A_I]$	real and imaginary parts of aerodynamic matrix, respectively

[E]	stiffness matrix
ρ	fluid density
s	reference length
b	reference semichord length
$\{q\}$	generalized coordinates

All matrices in eq. (1) are of order $n \times (n+r)$, that is, n structural modes and r active controls. Equation (1) can therefore be written as

$$\{F\} = \left(-\omega^2 \left[[B_s|B_c] + \pi\rho b^4 s([A_{R,s}|A_{R,c}] + i[A_{I,s}|A_{I,c}]) \right] + [E_s|E_c] \right) \left\{ \begin{array}{c} q \\ q_c \end{array} \right\}$$
(2)

where

$$\{\bar{q}\} = \left\{ \begin{array}{c} q \\ q_c \end{array} \right\}$$
(3)

Assume a control law of the form

$$\{q_c\} = [T]\{q\}$$
(4)

where [T] is a $r \times n$ matrix representing the transfer functions of the control law. The matrix [T] is therefore, in general, a function of the Laplace variable s. By substituting eq. (4) into eq. (2), the following equation is obtained:

$$\{F\} = \left(-\omega^2 \left[[B_s] + [B_c][T] + \pi\rho b^4 s([A_{R,s}] + [A_{R,c}][T] + i[A_{I,s}] + i[A_{I,c}][T]) \right] + [E_s] + [E_c][T] \right)\{q\}$$
(5)

It is shown in Nissim (1971 and 1977) that the work P done per cycle of oscillation by the system on its surroundings is given by

$$P = \frac{\pi \rho b^4 \omega^2 s}{2} \lfloor q_0^* \rfloor$$

$$\times \left[-\left([A_{I,s}] + [A_{I,s}]^T + [A_{I,c}][T] \right.\right.$$

$$\left. + [T^*]^T [A_{I,c}]^T \right)$$

$$+ i \left(\frac{[B_c][T] - [T^*]^T [B_c]^T}{\pi \rho b^4 s} \right.$$

$$+ [A_{R,s}] - [A_{R,s}]^T + [A_{R,c}][T]$$

$$\left.\left. - [T^*]^T [A_{R,c}]^T \right) \right] \{q_0\}$$

(6)

where

$$\{q\} = \{q_0\} e^{i\omega t}$$ (7)

It is also shown in Nissim (1977) that if [U] is defined to represent the expression within the square brackets in eq. (6), that is

$$[U] = \left[-\left([A_{I,s}] + [A_{I,s}]^T + [A_{I,c}][T] \right.\right.$$

$$\left. + [T^*]^T [A_{I,c}]^T \right)$$

$$+ i \left(\frac{[B_c][T] - [T^*]^T [B_c]^T}{\pi \rho b^4 s} + [A_{R,s}] \right.$$

$$- [A_{R,s}]^T + [A_{R,c}][T]$$

$$\left.\left. - [T^*]^T [A_{R,c}]^T \right) \right]$$

(8)

so that

$$P = \frac{\pi^2 \rho b^4 \omega^2 s}{2} \lfloor q_0 * \rfloor [U] \{q_0\}$$ (9)

then, by taking the eigenvalues of [U], that is, by solving

$$\lambda\{\eta\} = [U]\{\eta\}$$ (10)

P can be reduced to the form

$$P = \frac{\pi^2 \rho b^4 \omega^2 s}{2} \left[\lambda_1 \left(\xi_{R1}^2 + \xi_{I1}^2 \right) + \lambda_2 \left(\xi_{R2}^2 + \xi_{I2}^2 \right) \right.$$

$$\left. + \ldots + \lambda_n (\xi_{Rn}^2 + \xi_{In}^2) \right]$$

(11)

where λ_i is the ith eigenvalue of eq. (10), necessarily real since [U] is Hermitian, and ξ_R and ξ_I are defined by

$$\{q_0\} = [Q_R + iQ_I]\{\xi_R + i\xi_I\}$$ (12)

The columns of the square matrices $[Q_R]$ and $[Q_I]$ are the real and imaginary parts of the eigenvectors of eq. (10). The vector $\{\xi_R + i\xi_I\}$ contains the generalized modal coordinates of the transformation defined by eq. (12).

It should be noted that if all the λs in eq. (11) are positive, the system is stable (dissipative), irrespective of the responses represented by the different ξ values. If, however, one or more of the λs assumes a negative value, the system may become unstable if the ξ responses are such that P becomes negative. If one wishes to ensure stability irrespective of the responses of the system, all the λ values must be made positive.

In the following, it is desired to determine the contribution of the out-of-balance inertial terms independent of the aerodynamic terms (which are dependent on the flight configurations), and, therefore, consider the following expression for [U]:

$$[U] = i[B_c][T] - i[T^*]^T [B_c]^T$$ (13)

where the work done by the inertial out-of-balance terms is given by

$$P = \frac{\pi \omega^2}{2} \lfloor q_0^* \rfloor [U]\{q_0\}$$ (14)

Object of Analytical Work

The object of the following work is three-fold:

1. To determine a control matrix [T] that will ensure stability, that is, so that all the λ eigenvalues are positive.

2. To determine the effect of mass unbalance on the λs using the aerodynamic energy transfer function matrix [T].

3. To determine the possible compatibility between (1) and (2) above.

4

DETERMINATION OF [T] THAT ENSURES STABILITY OF MASS-UNBALANCED CONTROL SYSTEM

Basic Equations

Assume a two-dimensional strip performs pitch–plunge oscillations with activated L.E.–T.E. control surfaces.

Let

$$\{q_c\} = \left\{ \begin{array}{c} \beta \\ \delta \end{array} \right\} = [T] \left\{ \begin{array}{c} h/b \\ \alpha \end{array} \right\} \qquad (15)$$

where β is the L.E. rotation, positive nose down, and δ is the T.E. rotation, positive T.E. down. The deformations h and α indicate plunge (positive down) and pitch (positive nose up, Fig. 1). The parameter b denotes the semichord length of the 2-D wing.

Denote

$$[B_c] = \left[\begin{array}{cc} b_{11} & b_{12} \\ b_{21} & b_{22} \end{array} \right] \qquad (16)$$

where some detailed derivations for the different b_{ij} terms can be found in appendixes A and B. Let [T], for any value of frequency, be given by

$$[T] = \left[\begin{array}{cc} c_{11} + id_{11} & c_{12} + id_{12} \\ c_{21} + id_{21} & c_{22} + id_{22} \end{array} \right] \qquad (17)$$

Substituting eqs. (16) and (17) into eq. (13) one obtains, after some rearrangements, the following equation for [U]:

$$[U] = - \left[\begin{array}{c} 2(b_{11}d_{11} + b_{12}d_{21}) \\ \\ -i(b_{21}c_{11} + b_{22}c_{21} - b_{11}c_{12} - b_{12}c_{22}) \\ + (b_{21}d_{11} + b_{22}d_{21} + b_{11}d_{12} \\ + b_{12}d_{22}) \end{array} \right.$$

$$\left. \begin{array}{c} i(b_{21}c_{11} + b_{22}c_{21} - b_{11}c_{12} - b_{12}c_{22}) \\ + (b_{11}d_{12} + b_{12}d_{22} + b_{21}d_{11} \\ + b_{22}d_{21}) \\ \\ 2(b_{21}d_{12} + b_{22}d_{22}) \end{array} \right] \qquad (18)$$

It should be noted (see eqs. (2) and (15) to (17)) that for the case of an L.E. control only (that is when $\delta = 0$)

$$b_{12} = b_{22} = 0$$

and also

$$c_{21} = d_{21} = c_{22} = d_{22} = 0$$

Similarly, for the case of a T.E. control only (that is when $\beta = 0$)

$$b_{11} = b_{21} = 0$$

and also

$$c_{11} = d_{11} = c_{12} = d_{12} = 0$$

The characteristic equation for the determination of the eigenvalues λ of matrix [U], as given by eq. (13), is obtained from

$$|\lambda I - U| = 0$$

That is,

$$\lambda^2 + 2\lambda(b_{11}d_{11} + b_{12}d_{21} + b_{21}d_{12} + b_{22}d_{22})$$
$$+ 4(b_{11}d_{11}b_{21}d_{12} + b_{11}d_{11}b_{22}d_{22}$$
$$+ b_{12}d_{21}b_{21}d_{12} + b_{12}d_{21}b_{22}d_{22})$$
$$- (b_{11}d_{12} + b_{12}d_{22} + b_{21}d_{11} + b_{22}d_{21})^2$$
$$- (b_{21}c_{11} + b_{22}c_{21} - b_{11}c_{12} - b_{12}c_{22})^2 = 0$$
$$(19)$$

which can be rearranged to yield

$$\lambda^2 + 2\lambda(b_{11}d_{11} + b_{12}d_{21} + b_{21}d_{12} + b_{22}d_{22})$$
$$+ 4(b_{11}d_{11}b_{22}d_{22} + b_{12}d_{21}b_{21}d_{12})$$
$$- (b_{11}d_{12} - b_{21}d_{11})^2 - (b_{12}d_{22} - b_{22}d_{21})^2$$
$$- 2(b_{11}d_{12} + b_{21}d_{11})(b_{12}d_{22} + b_{22}d_{21})$$
$$- (b_{21}c_{11} + b_{22}c_{21} - b_{11}c_{12} - b_{12}c_{22})^2 = 0$$
$$(20)$$

Equation (20) forms the basis for the stability investigations presented in the following sections.

The Case of T.E. Control Only

To simplify the study of eq. (20), consider first the case of an activated T.E. only. In this case,

$$b_{11} = b_{21} = c_{11} = c_{12} = d_{11} = d_{12} = 0 \qquad (21)$$

Substituting eq. (21) into the characteristic eq. (20), one obtains

$$\lambda^2 + 2\lambda(b_{12}d_{21} + b_{22}d_{22})$$
$$-(b_{12}d_{22} - b_{22}d_{21})^2 - (b_{22}c_{21} - b_{12}c_{22})^2 = 0$$
$$(22)$$

Remembering that if λ_1, and λ_2 are the two roots of eq. (22), then

$$\lambda_1 + \lambda_2 = -2(b_{12}d_{21} + b_{22}d_{22}) \qquad (23)$$

and

$$\lambda_1\lambda_2 = -(b_{12}d_{22} - b_{22}d_{21})^2$$
$$-(b_{22}c_{21} - b_{12}c_{22})^2 \qquad (24)$$

the following conclusions result from eq. (22):

1. Because the constant element (independent of λ) is always negative (or at best equal to zero), there will always be a positive root λ_1 and a negative root λ_2.

2. The elements c_{21}, c_{22} do not affect the sum $(\lambda_1 + \lambda_2)$, but they do <u>reduce</u> the constant element, thus implying that while they increase the value of λ_1, they lead to a decrease in λ_2 by an equal amount.

3. Because for an unbalanced T.E. control, b_{12} and b_{22} are both positive (see appendix A), $\lambda_1 > -\lambda_2$ if d_{21} or d_{22} or both are negative so as to cause (see eq. (23))

$$b_{12}d_{21} + b_{22}d_{22} < 0 \qquad (25)$$

4. For the absolute value of λ_2 to be as small as possible while increasing λ_1 (to minimize the unstable root and maximize the stable one) without changing the control unbalance, one should aim at letting (see eq. (24))

$$c_{21} = c_{22} = 0 \quad \text{or} \quad \frac{c_{21}}{c_{22}} = \frac{b_{12}}{b_{22}}$$
$$\text{with } d_{21} < 0, \ d_{22} < 0 \qquad (26)$$

5. The optimum control law using the above criteria for inertially unbalanced T.E. stability is such that it satisfies eq. (26) above and <u>also</u> satisfies the equation

$$\frac{d_{22}}{d_{21}} = \frac{b_{22}}{b_{12}} \qquad (27)$$

making $\lambda_1\lambda_2 = 0$ (see eq. (24))

6. Equations (26) and (27) ensure that $\lambda_1 > 0$ (thus is stabilizing) while keeping $\lambda_2 = 0$ (and therefore, λ_2 does not contribute to instability). Note that λ_1 in this case assumes the value

$$\lambda_1 = -2(b_{12}d_{21} + b_{22}d_{22})$$

or, after substituting eq. (27)

$$\lambda_1 = -\left(2b_{22}d_{22} + 2\frac{b_{12}^2}{b_{22}}d_{22}\right)$$

$$\lambda_1 = -2b_{22}d_{22}\left(1 + \frac{b_{12}^2}{b_{22}^2}\right) \qquad (28)$$

The Case of L.E. Control Only

Following the above analysis for the case of the T.E. control only, a similar analysis will be performed for the case of L.E. control only. Hence, in this case, one can write

$$b_{12} = b_{22} = c_{21} = c_{22} = d_{21} = d_{22} = 0 \qquad (29)$$

Substituting eq. (29) into eq. (20) the following characteristic equation is obtained

$$\lambda^2 + 2\lambda(b_{11}d_{11} + b_{21}d_{12}) - (b_{11}d_{12} - b_{21}d_{11})^2$$
$$-(b_{21}c_{11} - b_{11}c_{12})^2 = 0$$
$$(30)$$

Equation (30) is similar in form to eq. (22), and the following similar conclusions can be drawn:

1. Because the constant element, which is independent of λ, is always negative, there will always be a positive root λ_1 and a negative root λ_2.

2. The elements c_{11} and c_{12} do not affect the sum $\lambda_1 + \lambda_2$, but they do reduce the constant element, thus causing an increase in the value of λ_1 while decreasing λ_2 by an equal amount.

3. Because an unbalanced L.E. control yields (shown in appendix A) positive b_{11} and negative b_{21}, the value of λ_1 will be larger than the absolute value of λ_2, that is $\lambda_1 > -\lambda_2$ if $d_{12} > 0$ or if $d_{11} < 0$ (or both conditions), so as to cause

$$[b_{11}d_{11} + b_{21}d_{12}] < 0 \qquad (31)$$

4. For the absolute of λ_2 to be as small as possible, while increasing λ_1 (to minimize the unstable root and maximize the stable one), without changing the control unbalance, one should aim at letting

$$c_{11} = c_{12} = 0 \left(\text{or } \frac{c_{12}}{c_{11}} = \frac{b_{21}}{b_{11}}\right)$$
$$d_{11} < 0, d_{12} > 0 \qquad (32)$$

5. The optimum control law based on the above criteria for inertially unbalanced L.E. control should have gains that satisfy eq. (32) and also satisfy the equation

$$\frac{d_{11}}{d_{12}} = \frac{b_{11}}{b_{21}} \qquad (33)$$

6. Equations (32) and (33) ensure that $\lambda_1 > 0$ (the stabilizing root) while keeping $\lambda_2 = 0$. Therefore, λ_2 does not contribute to instability. Note that λ_1 in this case assumes the value

$$\lambda_1 = -2(b_{11}d_{11} + b_{21}d_{12})$$

or, after substituting eq. (33)

$$\lambda_1 = -2b_{11}d_{11} - 2b_{21}d_{11}\frac{b_{21}}{b_{11}}$$

or

$$\lambda_1 = -2b_{11}d_{11}\left(1 + \frac{b_{21}^2}{b_{11}^2}\right) \qquad (34)$$

The Case of L.E.–T.E. Controls

The characteristic eq. (20) includes terms associated with L.E. control only, terms associated with T.E. control only, and <u>also</u> coupling terms between L.E. and T.E. controls. If the optimum control law conditions derived earlier for the L.E. (alone) system and T.E. (alone) system are applied to eq. (20), they ensure that:

1. The sum of $(\lambda_1 + \lambda_2) > 0$ since

$$(b_{11}d_{11} + b_{12}d_{21} + b_{21}d_{12} + b_{22}d_{22}) < 0 \quad (35)$$

2. All the negative quadratic terms that appear in the constant term in eq. (20) vanish, leaving the following coupling terms:

$$4[b_{11}d_{11}b_{22}d_{22} + b_{12}d_{21}b_{21}d_{12}]$$
$$- 2(b_{11}d_{12} + b_{21}d_{11})(b_{12}d_{22} + b_{22}d_{21})$$

Considering eqs. (26) and (32), and remembering that b_{11}, b_{12}, and b_{22} are all positive, while b_{21} is negative, it follows that both terms within the square bracket are positive (they add up) and the product terms end up being positive, thus <u>adding</u> to the square bracketed term. Also, within each of the parentheses forming the product, the terms <u>add</u> up so that the result is positive.

3. Based on conclusions (1) and (2) above, it follows that the optimum L.E. (alone) control law, and the optimum T.E. (alone) control law, yield a combined L.E.–T.E. control law with positive λ_1 <u>and positive λ_2</u>. Hence, the combined L.E.–T.E. control law will always be stabilizing from the point of view of inertial unbalance.

There remains to determine at this stage the compatibility between the unbalanced inertial stability requirements and those required by the aerodynamic energy method to stabilize the system as a result of acting aerodynamic forces.

Summary of Results

The very interesting results obtained so far are reiterated before proceeding to deal with their compatibility with the aerodynamic control laws:

1. Both L.E. alone and T.E. alone mass-unbalanced control systems always lead to inertial instabilities (or neutral stability at best), irrespective of the control laws employed. The best control law for these single control surface systems may reduce these instabilities to neutrally stable oscillations.

2. The combined L.E.–T.E. control system is shown to be much more powerful than any of its comprising components. With a proper control law, the mass-unbalance terms can be made to contribute to the stability of the system, irrespective of its characteristics and its responses.

COMPATIBILITY BETWEEN AERODYNAMIC AND INERTIAL CONTROL LAWS

Aerodynamic Energy Control Law

The basic aerodynamic energy L.E.–T.E. control law requires the matrix [T] to assume the form

$$[T] = \begin{bmatrix} t_{11} & t_{12} \\ t_{21} & t_{22} \end{bmatrix}$$

$$[T] = \begin{bmatrix} a_{11} + ie_{11} & \\ & a_{22} + ie_{22} \end{bmatrix} \begin{bmatrix} -1 & 1 \\ 1 & 0.7 \end{bmatrix} \qquad (36)$$

where a_{ii} terms can assume either positive or negative values, and the e_{ii} terms must be positive for aerodynamic stabilization (Nissim 1977). The constant terms in the matrix in eq. (36) were obtained in Nissim (1977) using numerical optimization, maximizing the aerodynamic energy eigenvalues over a whole range of subsonic Mach numbers. Note that when $a_{11} = e_{11} = 0$, eq. (36) yields a T.E. system, and similarly, when $a_{22} = e_{22} = 0$, eq. (36) yields an L.E. system. Note also that ratios t_{11}/t_{12} and t_{22}/t_{21} are constant. In the following a comparison is made between the aerodynamic control law given in eq. (36) and the inertial control law given in eq. (17), repeated here for the sake of clarity.

$$[T] = \begin{bmatrix} c_{11} + ia_{11} & c_{12} + id_{12} \\ c_{21} + id_{21} & c_{22} + id_{22} \end{bmatrix}$$

It is possible to vary these ratios between the t terms by changing the first column $\lfloor -1 \quad 1 \rfloor^T$ in eq. (36) relative to the second column. Such a variation may be considered if one is required to satisfy (or nearly satisfy) the relations in eqs. (24), (25), (30), and (31). If this is done, aerodynamic performance may be somewhat degraded. Therefore, relative changes in the first (or second) column of eq. (36) can be made during the design stage, when the mass unbalance detrimental effects need be overcome. In the following, the compatibility between eq. (36) and eqs. (24), (25), (30), and (31) is studied for the T.E. control system and for the L.E. control system. The results pertaining to an L.E.-T.E. control system follow the results of the preceeding two separate systems.

Compatibility Between Inertial and Aerodynamic Damping for a T.E. System

Equations (26) and (27) require that

$$\frac{c_{22}}{c_{21}} = \frac{d_{22}}{d_{21}} = \frac{b_{22}}{b_{12}} \tag{37}$$

Eq. (36) indicates that the first equality in eq. (37) is always satisfied, that is

$$\frac{c_{22}}{c_{21}} = \frac{d_{22}}{d_{21}} \tag{38}$$

irrespective of the relative values between the two columns in eq. (36). As shown in appendix A, eq. (A-8)

$$\frac{b_{22}}{b_{12}} > 1 \tag{39}$$

with both b_{22} and b_{12} being positive, for unbalanced T.E. control surfaces. The b_{22}/b_{12} ratio will be slightly larger than 1 for completely unbalanced T.E. control surface and can be made to tend to infinity for a statically balanced T.E. control (see eq. (A-9)). The statically balanced T.E. case is of little interest because in this case $b_{12} = 0$, and b_{22} is very small, thus yielding very small numerical values for λ that can be ignored, considering the structural damping of the system.

It follows from the above discussion that the value of 0.7 in the second column may need to be increased (relative to 1 in the first column) to a value somewhat larger than 1. The actual value can be determined in the design stage should such a need arise, when considering a specific numerical system. It can be readily shown that increasing the 0.7 gain moves the single sensor for the T.E control system further downstream (along the chord) than the 65 percent chord point associated with the 0.7 relative gain (Mukhopadhyay and others, 1981).

In eq. (26) both d_{21} and d_{22} must be negative. This requirement corresponds to e_{22} assuming negative values, and it therefore relates to the case where the resulting aerodynamic forces have a detrimental effect on stability. Hence, at the region of flutter, aerodynamic and inertial dampings are not compatible. This is a very important new result. Because flutter occurs at relatively low structural frequencies, a design should aim at producing a transfer function that yields:

1. Large positive values of e_{22} around the flutter frequency (eq. 36)

2. Negative values for e_{22} at high frequencies

3. Value of a_{22} that tends to zero at high frequencies (unless eqs. (26) and (27) are completely satisfied)

4. Value of e_{22} that tends to zero (with e_{22} being negative) at high frequencies, because there is no desire to control the very high frequency modes.

Compatibility Between Inertial and Aerodynamic Damping for an L.E. System

Equations (32) and (33) require that

$$\frac{c_{11}}{c_{12}} = \frac{d_{11}}{d_{12}} = \frac{b_{11}}{b_{21}} \qquad (40)$$

Eq. (36) indicates that the first equality in eq. (40) is always satisfied, that is

$$\frac{c_{11}}{c_{12}} = \frac{d_{11}}{d_{12}} \qquad (41)$$

irrespective of the relative values between the two columns in eq. (36). As shown in appendix A (see for example eq. (A-10)),

$$\left| \frac{b_{11}}{b_{21}} \right| > 1 \qquad (42)$$

for a mass-unbalanced L.E. control. As the control is balanced, the above ratio decreases until it reaches the value of zero for mass-balanced L.E. control. Furthermore, b_{11} is always positive (or zero when balanced), and b_{21} is always negative, so that b_{11}/b_{21} is always negative. From eq. (36) it can be seen that d_{11}/d_{12} (and therefore c_{11}/c_{12} by virtue of eq. (41)) is equal to -1. If the L.E. control is totally unbalanced, it is possible that the 1 in the second column of eq. (36) needs to be decreased. If $|b_{11}/b_{21}| < 1$ (for a partially balanced L.E. control), then it is possible the above value of 1 needs to be increased. Here again, the actual value can be determined later in the design stage, when considering a specific numerical system.

Equation (32) requires that d_{11} be negative and d_{12} be positive. Equation (36) shows that this requirement is fully met when e_{11} is positive. Hence, it can be seen that there exists a compatibility between the aerodynamic damping and the inertial damping. Hence, the L.E. control surface transfer function should aim to yield:

1. Positive values of e_{11} over a frequency range that spans the flutter frequency and extends to very high frequencies.

2. Value of a_{11} that tends to zero at high frequencies (unless eqs. (32) and (33) are completely satisfied).

3. Value of e_{11} that tends to zero (with e_{11} being positive) at high frequencies, because there is no desire to control very high frequency modes.

GENERALIZATION OF RESULTS FOR A REALISTIC WING STRIP

The analysis in appendix A that yields the matrix $[B_c]$ essentially assumes a rigid rectangular wing strip, performing pitch–plunge oscillations. A more realistic representation of the oscillation of a wing strip would allow the strip to rotate about its chordwise section, while performing the plunge motion. In addition, variations in both angle of attack and chord lengths along the strip always exist and their effects on the $[B_c]$ matrix need to be investigated. This latter investigation is important because the conclusions reached for control laws aimed at coping with mass-unbalanced control surfaces depend heavily on both the signs and relative sizes of the $[B_c]$ matrix.

The analysis of such a generalized wing strip is carried out in appendix B. The results yield the following $[B_c]$ matrix (see eq. (B-12)):

$$[B_c] = Mb_R^2 \left[\begin{array}{c} \bar{M}_L \left[1 + \left(\dfrac{h_y}{\bar{h}_R} \right) \bar{y}_{GL} + b_y \bar{y}_{GL} \right] \bar{x}_{GL} \\ \hline \bar{M}_L \left[1 + \left(\dfrac{\bar{\alpha}_y}{\alpha_R} \right) \bar{y}_{GL} + 2 b_y \bar{y}_{GL} \right] \times \\ \left[-(\bar{r}_{G\beta}^2 + \bar{x}_{GL}^2) + (\bar{x}_L + 0.4)\bar{x}_{GL} \right] \end{array} \right.$$

$$\left. \begin{array}{c} \bar{M}_T \left[1 + \left(\dfrac{h_y}{\bar{h}_R} \right) \bar{y}_{GT} + b_y \bar{y}_{GT} \right] \bar{x}_{GT} \\ \hline \bar{M}_T \left[1 + \left(\dfrac{\bar{\alpha}_y}{\alpha_R} \right) \bar{y}_{GT} + 2 b_y \bar{y}_{GT} \right] \times \\ \left[(r_{G\delta}^2 + \bar{x}_{GT}^2) + (\bar{x}_T + 0.4)\bar{x}_{GT} \right] \end{array} \right]$$

where M is the mass of the wing strip including the control surfaces (see eq. B-10).

$$\bar{M}_L = \frac{M_L}{M}$$
$$\bar{M}_T = \frac{M_T}{M} \qquad (43)$$

where M_L and M_T are the masses of the L.E. and T.E. control surfaces, respectively. The parameters h_y, $\bar{\alpha}_y$, and b_y are defined by

$$h_y = \frac{\partial h}{\partial y} = \text{const}$$

9

$$\bar{\alpha}_y = \frac{\partial \alpha}{\partial(y/b_R)} = \text{const}$$

$$b_y = \frac{\partial b}{\partial y} = \text{const}$$

where b_R denotes the strip's reference semichord length. Suffix R relates to the reference section (see figure in appendix B), and $\bar{h}_R$, $\bar{y}_{GL}$, and $\bar{y}_{GT}$ denote

$$\bar{h}_R = h_R/b_R$$

$$\bar{y}_{GL} = y_{GL}/b_R$$

$$\bar{y}_{GT} = y_{GT}/b_R$$

The parameters y_{GL} and y_{GT} denote the spanwise distances from the reference section of the center of gravity of the L.E. and T.E. control surfaces, respectively.

It should be noted that the effect of the generalized strip on the $[B_c]$ matrix can be large since $h_y/\bar{h}_R$ and $\bar{\alpha}_y/\alpha_R$ can assume large numerical values, with either positive or negative signs. It appears, therefore, that no single control law can stabilize the generalized strip unless the reference chord is chosen such that

$$\bar{y}_{GL} = \bar{y}_{GT} = 0 \qquad (44)$$

When eq. (44) is satisfied, the expression for $[B_c]$ reduces to the simple 2-D model case except for the mass ratio terms. Therefore, all the conclusions reached for the 2-D pitch–plunge strip apply to the generalized strip, provided eq. (44) is satisfied. Hence, we reach the following very important conclusions:

1. The spanwise reference section of an active strip should be chosen such that it passes through the center of gravity of the control surface.

2. If both L.E. and T.E. control surfaces are activated along the same strip, these two control surfaces should be aligned so that their centers of gravity lie along the same spanwise reference section.

3. If a similar analysis is performed for the aerodynamic forces, based on 2-D aerodynamics, the reference section should pass through the center of area of the generalized strip.

4. For best control of both inertial and aerodynamic destabilizing forces, the inertial reference section described in item (2) above should be made to pass through the center of area

of the wing mentioned in (3) above. Uniform wing and control surfaces do yield such a congruency.

NUMERICAL EXAMPLE AND RESULTS

A mathematical model of the YF-17 aircraft (Fig. 1) is used to test some of the results obtained in the present work. The available mathematical model allows for two activated control surfaces: one leading-edge control and one trailing-edge control. (Hwang and others, 1978, gives more details relating to the mathematical model.) However, no data is available regarding the alignment of the center of gravity of L.E. and T.E. controls, and therefore, deviations from some of the conclusions for the 2-D strip should be expected. To keep the focus of this work on the effects of mass unbalance on the stability of an active control system, no flutter calculations are made, and the system is tested for zero dynamic pressure. This means, in essence, that eq. (1) is solved for the case where

$$[A_R + iA_I] = 0 \text{ and } \{F\} = 0$$

The resulting equation reduces, in effect, to a vibration problem involving elastic and inertia forces only, with inertial coupling terms between activated control surfaces and structural degrees of freedom. This equation can be brought to the canonical form of an eigenvalue problem, the solution of which yields the state of stability of the system. All the eigenvalues presented in the attached tables relate to the solution of eq. (1) under the aforementioned conditions. Hence, a negative real part of an eigenvalue means a stable structural degree of freedom, and a positive real part of an eigenvalue will mean an unstable structural degree of freedom. These eigenvalues should not be confused with the energy eigenvalues discussed earlier in this work.

Table 1 presents the eigenvalues for the 10 elastic modes, both for the open-loop case and the closed-loop case, using real transfer functions only (that is, using real values for t_{ii}). It can be seen that a single control surface is activated each time, and that the effect of this activation on the stability of the system is absolutely negligible. Table 2 presents similar results pertaining to the simultaneous activation of both L.E. and T.E. control surfaces. Hence, it can be concluded that for the specific example in hand, the real parts of the

transfer function have a negligible effect on the stability of the system. Table 3 presents results pertaining to the complex transfer function

$$a(\omega_n) = \frac{-4s^2}{s^2 + 4s + 4} \times \frac{\omega_n}{(s + \omega_n)} \qquad (45)$$

where s denotes the Laplace variable. This transfer function was chosen to simulate the imaginary component of t_{ii} because the computer program available for the solution of eq. (1) is constrained to transfer functions where the order of the polynomial in s of the numerator is less or equal to the order of the polynomial in s in the denominator. The value of ω_n was chosen to equal 50 to ensure some gain at high frequencies. It should be noted that $a(\omega_n)$ introduces the positive values of e_{ii}. Similarly, $-a(\omega_n)$ introduces the negative values of e_{ii}. Contributions of the real part of the transfer function are expected to be small, following the results presented in Tables 1 and 2. On the basis of the foregoing analysis, it is expected that the T.E. with $-a(50)$ and the L.E. with $a(50)$ will each yield the most stable system in relative terms, as far as mass-unbalance effects are concerned. Table 3 confirms the aforementioned expectations. Table 4 presents results for a combined L.E.–T.E. active system using the $a(50)$ transfer function. Here again, it can be seen that the most stable system is the one obtained using $\bar{t}_{11} = a(50)$ and $\bar{t}_{22} = -a(50)$, as predicted herein, where

$$\bar{t}_{ii} = a_{ii} + e_{ii}$$

At this point it should be stressed, once again, that the results of the present analysis, based on a general 2-D system, were applied to a YF-17 mathematical model with no knowledge of the degree of mass unbalance, control surfaces' center of gravity locations, or spanwise locations of the control surface centers of gravity. Nevertheless, the correlation between analysis and results is indeed impressive.

CONCLUSIONS

The study of the effects of mass-unbalanced control surfaces on the stability of the closed-loop system indicates that:

1. A single L.E. or a single T.E. mass-unbalanced control surface may lead to instability (or neutral stability) arising from inertial forces, irrespective of the control law used, because not all energy eigenvalues can be made to assume positive values.

2. The most efficient single L.E. or T.E. mass-unbalanced control surface can be made to yield a zero energy eigenvalue in addition to a positive eigenvalue, thus indicating the possibility of neutral stability (or an uncontrollable mode).

3. A combined L.E.–T.E. mass-unbalanced control system is shown to permit stabilization, irrespective of the mode of oscillation of the wing.

4. Inertial and aerodynamic control laws can be made compatible for an L.E. control system. Incompatibility exists, however, between aerodynamic and inertial control laws for a T.E. control system.

5. For mass-unbalanced stabilization to be insensitive to mode of oscillation for a continuous system like a wing surface, the sensor should be placed along a streamwise section that passes through the spanwise center of gravity of the control surface.

6. When two control surfaces are activated on one strip of the wing (like an L.E.–T.E. control system), the two control surfaces should be aligned so their spanwise centers of gravity lie on the same streamwise section, with the sensors placed along this section.

7. Results obtained herein suggest that the best geometrical arrangement for flutter suppression should aim at aligning the control surfaces' spanwise centers of gravity (section (6) above) with the spanwise centroid of the wing strip, where the control surfaces are located.

8. Numerical results relating to a YF-17 mathematical model appear to agree with the theoretical predictions based on the analysis made in the present work.

9. Results obtained herein can be used to stabilize elastic modes of large space structures by means of inertial forces.

APPENDIX   A
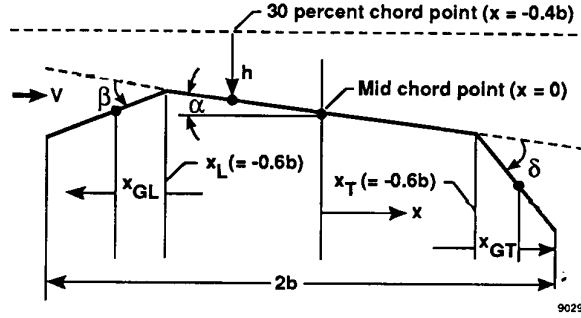# DERIVATION OF CONTROL SURFACE CROSS-INERTIA TERMS

Figure A1. A L.E.–T.E. Control System

The following derivation of control surface cross inertia terms is performed for a general configuration of a L.E.–T.E. system. Numerical estimates, however, will relate to 20 percent chord control surfaces.

The kinetic energy of the system described in the above sketch is given by:

$$K.E. = \frac{1}{2} \int_{-b}^{x_L} dm[\dot{h} + (x + 0.4b)\dot{\alpha} + (x_L - x)\dot{\beta}]^2 + \frac{1}{2} \int_{x_L}^{x_T} dm[\dot{h} + (x + 0.4b)\dot{\alpha}]^2$$

$$+ \frac{1}{2} \int_{x_T}^{b} dm[\dot{h} + (x + 0.4b)\dot{\alpha} + (x - x_T)\dot{\delta}]^2 \tag{A-1}$$

where x_L and x_T (shown in the figure) denote the x coordinates of the L.E. and T.E. hinge lines, respectively. The kinetic energy coupling terms with control surface deflections are given by

$$(K.E.)_c = \int_{-b}^{x_L} dm[(x + 0.4b)(x_L - x)\dot{\alpha}\dot{\beta} + (x_L - x)\dot{h}\dot{\beta}]$$

$$+ \int_{x_T}^{b} dm[(x + 0.4b)(x - x_T)\dot{\alpha}\dot{\delta} + (x - x_T)\dot{h}\dot{\delta}]$$

or

$$(K.E.)_c = m_L x_{GL} \dot{h}\dot{\beta} + m_T x_{GT} \dot{h}\dot{\delta}$$

$$+ \int_{-b}^{x_L} dm(x - x_L + x_L + 0.4b)(x_L - x)\dot{\alpha}\dot{\beta}$$

$$+ \int_{x_T}^{b} dm(x - x_T + x_T + 0.4b)(x - x_T)\dot{\alpha}\dot{\delta}$$

where m_L is the mass of the L.E. control surface, m_T is the mass of the T.E. control surface, x_{GL} is the distance from the hinge line of the center of gravity of the L.E. control, positive if upstream of the hinge line, and x_{GT} is the distance from the hinge line of the center of gravity of the T.E. control, positive if downstream of the hinge line.

The above equation can be integrated to yield the following form:

$$(K.E.)_c = m_L \frac{x_{GL}}{b} b^2 \frac{\dot{h}}{b} \dot{\beta} + m_T \frac{x_{GT}}{b} b^2 \frac{\dot{h}}{b} \dot{\delta} + [I_\delta + (x_T + 0.4b) m_T x_{GT}]\dot{\alpha}\dot{\delta}$$

$$+ [-I_\beta + (x_L + 0.4b) m_L x_{GL}]\dot{\alpha}\dot{\beta} \tag{A-2}$$

12

where

$$I_\delta = \int_{x_T}^{b} (x - x_T)^2 \, dm$$

$$I_\beta = \int_{-b}^{x_L} (x - x_L)^2 \, dm$$

and I_β and I_δ are the moment of inertia, about the control surface hinge line of the L.E. and T.E. controls, respectively.

Equation (A-2) can further be reduced to the following form:

$$(\text{K.E.})_c = m_L \bar{x}_{GL} b^2 \frac{h}{b} \dot{\beta} + m_T \bar{x}_{GT} b^2 \frac{h}{b} \dot{\delta} + m_T b^2 [(\bar{r}_{G\delta}^2 + \bar{x}_{GT}^2) + (\bar{x}_T + 0.4) \bar{x}_{GT}] \dot{\alpha} \dot{\delta}$$
$$+ m_L b^2 [-(\bar{r}_{GB}^2 + \bar{x}_{GL}^2) + (\bar{x}_L + 0.4) \bar{x}_{GL}] \dot{\alpha} \dot{\beta} \tag{A-3}$$

where $\bar{r}_{G\delta}$ and $\bar{r}_{G\beta}$ are the normalized radii of gyration (normalized with respect to the semichord length b), of the T.E. and L.E. control surfaces, respectively, about their respective control surface center of gravity points. The bar above the parameters x_{GL}, x_{GT}, x_L, and x_T indicates that the parameters are normalized with respect to the semichord length b.

The expression for the kinetic energy in eq. (A-3) is now differentiated as required by Lagrange's equations, to obtain the inertia terms, that is

$$\frac{d}{dt} \left(\frac{\partial (\text{K.E.})_c}{\partial (h/b)} \right) = m_L \bar{x}_{GL} b^2 \ddot{\beta} + m_T \bar{x}_{GT} b^2 \ddot{\delta}]$$

$$\frac{d}{dt} \left(\frac{\partial (\text{K.E.})_c}{\partial \dot{\alpha}} \right) = m_T b^2 \left[(\bar{r}_{G\delta}^2 + \bar{x}_{GT}^2) + (\bar{x}_T + 0.4) \bar{x}_{GT} \right] \ddot{\delta}$$
$$+ m_L b^2 \left[-(\bar{r}_{G\beta}^2 + x_{GL}^2) + (\bar{x}_L + 0.4) \bar{x}_{GL} \right] \ddot{\beta} \tag{A-4}$$

Equation (A-4) yields the following coupling mass matrix (with the h/b and α degrees of freedom):

$$[B_c] = \begin{bmatrix} m_L b^2 \bar{x}_{GL} & m_T b^2 \bar{x}_{GT} \\ m_L b^2 [-(\bar{r}_{G\beta}^2 + \bar{x}_{GL}^2) + (\bar{x}_L + 0.4) \bar{x}_{GL}] & m_T b^2 [(\bar{r}_{G\delta}^2 + x_{GT}^2) + (\bar{x}_T + 0.4) \bar{x}_{GT}] \end{bmatrix}$$

which can be reduced to

$$[B_c] = mb^2 \begin{bmatrix} \bar{m}_L \bar{x}_{GL} & \bar{m}_T \bar{x}_{GT} \\ m_L [-(\bar{r}_{G\beta}^2 + \bar{x}_{GL}^2) + (\bar{x}_L + 0.4) \bar{x}_{GL}] & \bar{m}_T [(\bar{r}_{G\delta}^2 + \bar{x}_{GT}^2) + (\bar{x}_T + 0.4) \bar{x}_{GT}] \end{bmatrix} \tag{A-5}$$

where m is the mass of the two-dimensional section, m_L and m_T are given by

$$\bar{m}_L = \frac{m_L}{m}$$

$$\bar{m}_T = \frac{m_T}{m} \tag{A-6}$$

Note: It should be noted that if $[B_c]$ is denoted by

$$[B_c] = \begin{bmatrix} b_{11} & b_{12} \\ b_{21} & b_{22} \end{bmatrix} \tag{A-7}$$

then eq. (A-5) indicates that b_{11} and b_{12} are always positive for mass unbalanced L.E. and T.E. control surfaces. For a 20 percent chord T.E. control, $\bar{x}_T = 0.6$ thus yielding positive values for b_{22} (which will be positive for all T.E. control surfaces of sizes less than 70 percent chord—that is for $x_T > -0.4$—namely for all practical cases). Note also that b_{22}/b_{12} will always be larger than 1, that is

$$\frac{b_{22}}{b_{12}} > 1 \tag{A-8}$$

For a 20 percent L.E. control surface $\bar{x}_L = -0.6$, thus yielding a negative value for b_{21} (which will remain negative for L.E. control surfaces of sizes less than 30 percent chord—that is for $\bar{x}_L < -0.4$—namely again—for all practical cases).

Numerical Example

To get some insight into the different values of the b_{ij} terms, the following example is presented. Consider 20 percent control surfaces (i.e., $\bar{x}_L = -0.6$, $\bar{x}_T = 0.6$) yielding the following values for $[B_c]$, (see eq. (A-5)):

$$[B_c] = mb^2 \begin{bmatrix} \bar{m}_L \bar{x}_{GL} & \bar{m}_T \bar{x}_{GT} \\ \bar{m}_L[-(\bar{r}_{G\beta}^2 + \bar{x}_{GL}^2) - 0.2\bar{x}_{GL}] & \bar{m}_T[(\bar{r}_{G\delta}^2 + \bar{x}_{GT}^2) + \bar{x}_{GT}] \end{bmatrix}$$

Note that in this case

$$\frac{b_{22}}{b_{12}} = 1 + \frac{\bar{r}_{G\delta}^2 + \bar{x}_{GT}^2}{x_{GT}} \tag{A-9}$$

and

$$\frac{b_{11}}{b_{21}} = \frac{\bar{x}_{GL}}{-0.2\bar{x}_{GL} - \bar{r}_{G\beta}^2 - \bar{x}_{GL}^2} \tag{A-10}$$

Assume also that the airfoil and control surfaces can be approximated to the homogeneous cross section shown below.
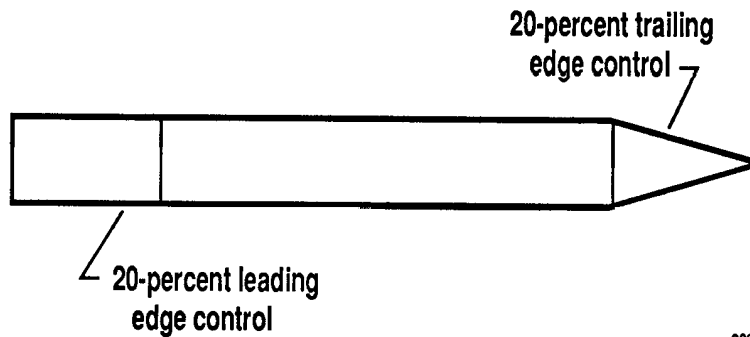
Figure A2. Schematic Approximation of L.E.–T.E. System

Under these conditions, it can be readily shown that

$$\bar{m}_L = 0.22 \qquad \bar{m}_T = 0.11$$
$$\bar{x}_{GL} = 0.2 \qquad \bar{x}_{GT} = 0.133$$
$$\bar{r}_{G\beta}^2 = 0.0133 \qquad \bar{r}_{G\delta}^2 = 0.00889$$

14

Hence,

$$[B_c] = mb^2 \begin{bmatrix} 0.22 \times 0.2 & 0.11 \times 0.133 \\ 0.22[-(0.0133 + 0.04) - 0.2 \times 0.2] & 0.11[0.00889 + 0.0178 + 0.133] \end{bmatrix}$$

or

$$[B_c] = mb^2 \begin{bmatrix} 0.044 & 0.01463 \\ -0.0205 & 0.01757 \end{bmatrix}$$

APPENDIX B
DERIVATION OF CROSS-INERTIA TERMS FOR A GENERALIZED WING
STRIP WITH CONTROL SURFACES

Figure B1. Generalized wing strip

Consider the wing strip shown above. An attempt will now be made to generalize the results obtained in appendix A to nonrectangular wing strips which exhibi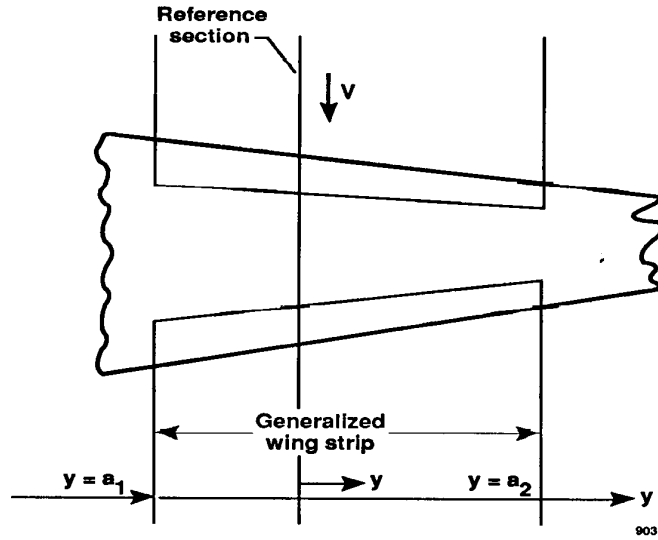t spanwise deformation in twist, together with rotation (about a chordwise axis) which results from the bending of the wing. This implies that the plunge h at the 30 percent chord location, the local angle of attack α and the local semichord length b along the strip of the wing can be allowed to vary along the span of the strip. It will now be assumed the above variation to be linear and having small derivatives (with respect to the spanwise coordinate y). That is, let

$$h = h_R + h_y y$$
$$\alpha = \alpha_R + \alpha_y y$$
$$b = b_R + b_y y \; ; \; b_y \ll 1 \tag{B-1}$$

where

$$h_y = \frac{\partial h}{\partial y} = \text{const along the strip}$$

$$\alpha_y = \frac{\partial \alpha}{\partial y} = \text{const along the strip}$$

$$b_y = \frac{\partial b}{\partial y} = \text{const along the strip} \tag{B-2}$$

and where suffix R relates to the reference section indicated in the sketch above.

Equation (A-3) can be made to be applicable to an infinitesimal strip. Assume that m_L and m_T in eq. (A-3) now denote local masses per unit span of the L.E. and T.E. control surfaces, respectively. Hence, the infinitesimal strip masses will be given by $m_L dy$ and $m_T dy$, and eq. (A-3) will now assume the following form (for the spanwise integration of the kinetic energy), that is

16

$$(\text{K.E.})_c = \int_{a_1}^{a_2} m_L(y)\,\bar{x}_{\text{GL}}\,b h \dot{\beta}\,dy + \int_{a_1}^{a_2} m_T(y)\,\bar{x}_{\text{GT}}\,b h \dot{\delta}\,dy$$

$$+ \int_{a_1}^{a_2} m_T(y)\,b^2\,[\,(\bar{r}_{G\delta}^2 + \bar{x}_{\text{GT}}^2) + (\bar{x}_T + 0.4)\bar{x}_{\text{GT}}\,]\,\dot{\alpha}\dot{\delta}\,dy$$

$$+ \int_{a_1}^{a_2} m_L(y)\,b^2\,[\,-(\bar{r}_{G\beta}^2 + \bar{x}_{\text{GL}}^2)$$

$$+ (\bar{x}_L + 0.4)\bar{x}_{\text{GL}}\,]\,\dot{\alpha}\dot{\beta}\,dy \qquad \text{(B-3)}$$

Assume also that the local control surfaces chords, relative to the wing chord are independent of the spanwise coordinate y, and that the control surface satisfies the following relations (see appendix A)

$$\bar{x}_L = \text{const}$$
$$\bar{x}_T = \text{const}$$
$$\bar{x}_{\text{GL}} = \text{const}$$
$$\bar{x}_{\text{GT}} = \text{const}$$
$$\bar{r}_{G\delta} = \text{const}$$
$$\bar{r}_{G\beta} = \text{const} \qquad \text{(B-4)}$$

Substituting eq. (B-1) into eq. (B-3) yields

$$(\text{K.E.})_c = \left[\int_{a_1}^{a_2} m_L(y)(b_R + b_y y)(\dot{h}_R + \dot{h}_y y)\,dy\right]\bar{x}_{\text{GL}}\,\dot{\beta} + \left[\int_{a_1}^{a_2} m_T(y)(b_R + b_y y)(\dot{h}_R + \dot{h}_y y)\,dy\right]\bar{x}_{\text{GT}}\,\dot{\delta}$$

$$+ \left[\int_{a_1}^{a_2} m_T(y)(b_R + b_y y)^2(\dot{\alpha}_R + \dot{\alpha}_y y)\,dy\right]\left[(\bar{r}_{G\delta}^2 + \bar{x}_{\text{GT}}^2) + (\bar{x}_T + 0.4)\bar{x}_{\text{GT}}\right]\dot{\delta}$$

$$+ \left[\int_{a_1}^{a_2} m_L(y)(b_R + b_y y)^2(\dot{\alpha}_R + \dot{\alpha}_y y)\,dy\right]\left[-(\bar{r}_{G\beta}^2 + \bar{x}_{\text{GL}}^2) + (\bar{x}_L + 0.4)\bar{x}_{\text{GL}}\right]\dot{\beta} \qquad \text{(B-5)}$$

Expanding eq. (B-5) and ignoring second order terms in b_y, one obtains

$$(\text{K.E.})_c = \left[\int_{a_1}^{a_2} m_L(y)(b_R \dot{h}_R + b_R \dot{h}_y y + b_y \dot{h}_R y + b_y \dot{h}_y y^2)\,dy\right]\bar{x}_{\text{GL}}\,\dot{\beta}$$

$$+ \left[\int_{a_1}^{a_2} m_T(y)(b_R \dot{h}_R + b_R \dot{h}_y y + b_y \dot{h}_R y + b_y \dot{h}_y y^2)\,dy\right]\bar{x}_{\text{GT}}\,\dot{\delta}$$

$$+ \left[\int_{a_1}^{a_2} m_T(y)(b_R^2 + 2b_R b_y y)(\dot{\alpha}_R + \dot{\alpha}_y y)\,dy\right]$$

$$\times [(\bar{r}_{G\delta}^2 + \bar{x}_{\text{GT}}^2) + (\bar{x}_T + 0.4)\bar{x}_{\text{GT}}]\dot{\delta}$$

$$+ \left[\int_{a_1}^{a_2} m_L(y)(b_R^2 + 2b_R b_y y)(\dot{\alpha}_R + \dot{\alpha}_y y)\,dy\right]$$

$$\times [-(\bar{r}_{G\beta}^2 + \bar{x}_{\text{GL}}^2) + (\bar{x}_L + 0.4)\bar{x}_{\text{GL}}]\dot{\beta}$$

which can be reduced to

$$(\text{K.E.})_c = [M_L b_R \dot{h}_R + M_L b_R \dot{h}_y y_{\text{GL}} + M_L b_y y_{\text{GL}} \dot{h}_R + M_L r_{yL}^2 b_y \dot{h}_y]\bar{x}_{\text{GL}}\,\dot{\beta}$$

$$+ [M_T b_R \dot{h}_R + M_T b_R \dot{h}_y y_{\text{GT}} + M_T b_y y_{\text{GT}} \dot{h}_R + M_T r_{yT}^2 b_y \dot{h}_y]\bar{x}_{\text{GT}}\,\dot{\delta}$$

$$+ [M_T b_R^2 \dot{\alpha}_R + M_T b_R^2 \dot{\alpha}_y y_{\text{GT}} + 2 M_T b_R b_y \dot{\alpha}_R y_{\text{GT}} + 2 M_T b_R b_y \dot{\alpha}_y r_{yT}^2]$$

$$\times [(\bar{r}_{G\delta}^2 + \bar{x}_{\text{GT}}^2) + (\bar{x}_T + 0.4)\bar{x}_{\text{GT}}]\dot{\delta} + [M_L b_R^2 \dot{\alpha}_R + M_L b_R^2 \dot{\alpha}_y y_{\text{GL}} + 2 M_L b_R b_y \dot{\alpha}_R y_{\text{GL}} + 2 M_L b_R b_y \dot{\alpha}_y r_{yL}^2]$$

$$\times [-(\bar{r}_{G\beta}^2 + \bar{x}_{\text{GL}}^2) + (\bar{x}_L + 0.4)\bar{x}_{\text{GL}}]\dot{\beta} \qquad \text{(B-6)}$$

where M_L and M_T denote the masses of the L.E. and T.E. control surfaces, respectively, and r_{yL}, r_{yT} denote the radii of inertia about the reference streamwise section of the L.E. and T.E. control surfaces, respectively. Without affecting the generality of the results, assume that a relationship exists between h_y and h_R, α_y and α_R (like the relationship existing during a modal oscillation), such that

$$\frac{\dot{h}_y}{\dot{h}_R} = \frac{h_y}{h_R}$$

$$\frac{\dot{\alpha}_y}{\dot{\alpha}_R} = \frac{\alpha_y}{\alpha_R} \tag{B-7}$$

so that eq. (B-6) can be written in the form

$$
\begin{aligned}
(\text{K.E.})_c = {} & M_L b_R^2 \left[1 + \left(\frac{h_y}{h_R} \right) y_{GL} + \left(\frac{b_y}{b_R} \right) y_{GL} + b_y \left(\frac{r_{yL}}{b_R} \right)^2 \left(\frac{h_y}{h_R} \right) \right] \bar{x}_{GL} \left(\frac{\dot{h}_R}{b_R} \right) \dot{\beta} \\
& + M_T b_R^2 \left[1 + \left(\frac{h_y}{h_R} \right) y_{GT} + \left(\frac{b_y}{b_R} \right) y_{GT} + b_y \left(\frac{r_{yT}}{b_R} \right)^2 \left(\frac{h_y}{h_R} \right) \right] \bar{x}_{GT} \left(\frac{\dot{h}_R}{b_R} \right) \dot{\delta} \\
& + M_T b_R^2 \left[1 + \left(\frac{\alpha_y}{\alpha_R} \right) y_{GT} + 2 \left(\frac{b_y}{b_R} \right) y_{GT} + 2 b_R b_y \left(\frac{\alpha_y}{\alpha_R} \right) \left(\frac{r_{yT}}{b_R} \right)^2 \right] \\
& \times \left[(\bar{r}_{G\delta}^2 + \bar{x}_{GT}^2) + (\bar{x}_T + 0.4) \bar{x}_{GT} \right] \dot{\alpha}_R \delta \\
& + M_L b_R^2 \left[1 + \left(\frac{\alpha_y}{\alpha_R} \right) y_{GL} + 2 \left(\frac{b_y}{b_R} \right) y_{GL} + 2 b_R b_y \left(\frac{\alpha_y}{\alpha_R} \right) \left(\frac{r_{yL}}{b_R} \right)^2 \right] \\
& \times \left[-(\bar{r}_{G\beta}^2 + \bar{x}_{GL}^2) + (\bar{x}_L + 0.4) \bar{x}_{GL} \right] \dot{\alpha}_R \dot{\beta} \tag{B-8}
\end{aligned}
$$

Assuming

$$\left(\frac{r_{yL}}{b_R} \right)^2 \ll 1 \quad ; \quad \left(\frac{r_{yT}}{b_R} \right)^2 \ll 1$$

one can neglect the second order terms in eq. (B-8) involving $b_y \left(\frac{r_{yL}}{b_R} \right)^2$ and $b_y \left(\frac{r_{yT}}{b_R} \right)^2$. Differentiating eq. (B-8), as specified by Lagrange's equations (see appendix A), one obtains the following $[B_c]$ matrix

$$
[B_c] = M b_R^2
\begin{bmatrix}
\bar{M}_L \left[1 + \left(\frac{h_y}{h_R} \right) y_{GL} + \left(\frac{b_y}{b_R} \right) y_{GL} \right] \bar{x}_{GL} & \bar{M}_T \left[1 + \left(\frac{h_y}{h_R} \right) y_{GT} + \left(\frac{b_y}{b_R} \right) y_{GT} \right] \bar{x}_{GT} \\
\hline
\bar{M}_L \left[1 + \left(\frac{\alpha_y}{\alpha_R} \right) y_{GL} + 2 \left(\frac{b_y}{b_R} \right) y_{GL} \right] \times & \bar{M}_T \left[1 + \left(\frac{\alpha_y}{\alpha_R} \right) y_{GT} + 2 \left(\frac{b_y}{b_R} \right) y_{GT} \right] \times \\
\left[-(\bar{r}_{G\beta}^2 + \bar{x}_{GL}^2) + (\bar{x}_L + 0.4) \bar{x}_{GL} \right] & \left[(\bar{r}_{G\delta}^2 + \bar{x}_{GT}^2) + (\bar{x}_T + 0.4) \bar{x}_{GT} \right]
\end{bmatrix}
\tag{B-9}
$$

where M is the mass of the strip and

$$\bar{M}_L = \frac{M_L}{M}$$

$$\bar{M}_T = \frac{M_T}{M} \tag{B-10}$$

The element inside the square matrix can be nondimensionalized by normalizing with respect to the reference chord, in the following manner:

18

Let

$$\bar{\alpha}_y = \frac{\partial \alpha}{\partial (y/b_R)}$$

$$\bar{h}_R = \bar{h}_R/b_R$$

$$\bar{y}_{GL} = y_{GL}/b_R$$

$$\bar{y}_{GT} = y_{GT}/b_R \tag{B-11}$$

Then eq. (B-9) can be written in the following form:

$$[B_c] = M b_R^2 \begin{bmatrix} \bar{M}_L \left[1 + \left(\dfrac{h_y}{\bar{h}_R} \right) \bar{y}_{GL} + b_y \bar{y}_{GL} \right] \bar{x}_{GL} & \bar{M}_T \left[1 + \left(\dfrac{h_y}{\bar{h}_R} \right) \bar{y}_{GT} + b_y \bar{y}_{GT} \right] \bar{x}_{GT} \\ \hline \bar{M}_L \left[1 + \left(\dfrac{\bar{\alpha}_y}{\alpha_R} \right) \bar{y}_{GL} + 2 b_y \bar{y}_{GL} \right] \times & \bar{M}_T \left[1 + \left(\dfrac{\bar{\alpha}_y}{\alpha_R} \right) \bar{y}_{GT} + 2 b_y \bar{y}_{GT} \right] \times \\ \left[-(\bar{r}_{G\beta}^2 + \bar{x}_{GL}^2) + (\bar{x}_L + 0.4) \bar{x}_{GL} \right] & \left[(\bar{r}_{G\delta}^2 + \bar{x}_{GT}^2) + (\bar{x}_T + 0.4) \bar{x}_{GT} \right] \end{bmatrix} \tag{B-12}$$

REFERENCES

[1] Mukhopadhyay, V., Newsom, J.R., and Abel, I., "A Method for Obtaining Reduced-Order Control Laws for High-Order Systems Using Optimization Techniques," NASA TP-1876, 1981.

[2] Newsom, J.R., "A Method for Obtaining Practical Flutter-Suppression Control Laws Using Results of Optimal Control Theory," NASA TP-1471, 1979.

[3] Newsom, J.R., Abel, I., and Dunn, H.J., "Application of Two Design Methods for Active Flutter Suppression and Wind-Tunnel Test Results," NASA TP-1653, 1980.

[4] Nissim, E., and Abel, I., "Development and Application of an Optimization Procedure for Flutter Suppression Using the Aerodynamic Energy Concept," NASA TP-1137, 1978.

[5] Mahesh, J.K., Stone, C.R., Garrard, W.L., and Dunn, H.J., "Control Law Synthesis for Flutter Suppression Using Linear Quadratic Gaussian Theory," AIAA J. Guidance and Control, Vol. 4, No. 4, July–Aug. 1981, pp. 415–422.

[6] Freymann, R., "Interactions Between an Aircraft Structure and Active Control Systems," AIAA J. Guid. Control and Dyn., Vol. 10, No. 5, Sept.–Oct. 1987, pp. 447–452.

[7] Nissim, E., "Flutter Suppression Using Active Controls Based on the Concept of Aerodynamic Energy," NASA TN D-6199, 1971.

[8] Nissim, E., "Recent Advances in Aerodynamic Energy Concept for Flutter Suppression and Gust Alleviation Using Active Controls," NASA TN D-8519, 1977.

[9] Hwang, C., Winther, B.A., and Mills, G.R., "Demonstration of Active Wing/Store Flutter Suppression Systems," AFFDL-TR-78-65, 1978.

TABLE 1. Variation With Single Control Mass Unbalance of
Complex Eigenvalues λ Using Real Transfer Function

R10		R11		R12		R13		R14	
λ_{Real}	$\lambda_{Imaginary}$	λ_{Real}	$\lambda_{Imaginary}$	λ_{Real}	$\lambda_{Imaginary}$	λ_{Real}	$\lambda_{Imaginary}$	λ_{Real}	$\lambda_{Imaginary}$
−0.1563E−12	0.3893E+03	−0.4707E−12	0.3884E+03	0.1066E−12	0.3906E+03	−0.2132E−13	0.3899E+03	−0.3055E−12	0.3888E+03
−0.1421E−12	0.3168E+03	−0.2842E−13	0.3094E+03	0.1847E−12	0.3249E+03	−0.5365E−12	0.3213E+03	0.7105E−13	0.3129E+03
−0.1137E−12	0.2671E+03	−0.3197E−13	0.2668E+03	0.4263E−13	0.2673E+03	0.3104E−12	0.2691E+03	−0.9948E−13	0.2649E+03
−0.3126E−12	0.2277E+03	−0.1616E−12	0.2277E+03	0.1172E−12	0.2277E+03	0.2034E−12	0.2278E+03	0.2558E−12	0.2276E+03
−0.2132E−12	0.1613E+03	−0.1279E−12	0.1613E+03	0.5258E−12	0.1613E+03	0.2842E−13	0.1613E+03	−0.5684E−13	0.1613E+03
0.1705E−12	0.1203E+03	0.1030E−12	0.1203E+03	0.2416E−12	0.1203E+03	−0.4832E−12	0.1203E+03	−0.1634E−12	0.1203E+03
−0.3411E−12	0.9351E+02	0.1151E−11	0.9319E+02	0.3439E−11	0.9384E+02	0.3979E−12	0.9357E+02	−0.6928E−12	0.9345E+02
0.9948E−13	0.8416E+02	0.1265E−11	0.8404E+02	−0.5471E−12	0.8427E+02	−0.3268E−11	0.8419E+02	0.2721E−11	0.8413E+02
0.1705E−12	0.4515E+02	0.4062E−11	0.4514E+02	0.5826E−12	0.4516E+02	−0.4952E−11	0.4517E+02	0.6297E−12	0.4513E+02
0.2842E−13	0.2908E+02	−0.5912E−11	0.2903E+02	−0.4743E−11	0.2913E+02	−0.8630E−11	0.2909E+02	−0.9603E−11	0.2907E+02

R10—Open Loop
R11-T.E. Only; $\hat{r}_{22} = 4$
R12-T.E. Only; $\hat{r}_{22} = -4$
R13-L.E. Only; $\hat{r}_{11} = 4$
R14-L.E. Only; $\hat{r}_{11} = -4$

TABLE 2. Variation With L.E.–T.E. Mass Unbalance of
Complex Eigenvalues λ Using Real Transfer Function

R15		R16		R17		R18	
λ_{Real}	$\lambda_{Imaginary}$	λ_{Real}	$\lambda_{Imaginary}$	λ_{Real}	$\lambda_{Imaginary}$	λ_{Real}	$\lambda_{Imaginary}$
0.1492E−12	0.3889E+03	−0.2700E−12	0.3880E+03	−0.2842E−13	0.3914E+03	0.5542E−12	0.3899E+03
−0.4690E−12	0.3140E+03	−0.4263E−13	0.3055E+03	0.7816E−12	0.3292E+03	−0.5087E−11	0.3211E+03
−0.4050E−12	0.2687E+03	−0.1137E−12	0.2648E+03	0.2842E−13	0.2695E+03	−0.6928E−12	0.2650E+03
0.3979E−12	0.2278E+03	0.6182E−12	0.2277E+03	−0.7105E−13	0.2277E+03	−0.2380E−12	0.2276E+03
−0.2387E−11	0.1613E+03	−0.8100E−12	0.1613E+03	0.7319E−12	0.1613E+03	−0.3979E−12	0.1613E+03
−0.1279E−12	0.1203E+03	0.8527E−13	0.1203E+03	0.1243E−11	0.1203E+03	−0.5116E−12	0.1203E+03
−0.2984E−12	0.9325E+02	−0.2540E−12	0.9313E+02	−0.4849E−12	0.9391E+02	0.3126E−12	0.9377E+02
0.1580E−10	0.8407E+02	0.5329E−11	0.8401E+02	−0.1023E−10	0.8430E+02	0.2323E−10	0.8425E+02
−0.1696E−11	0.4517E+02	0.4245E−11	0.4512E+02	−0.3924E−12	0.4518E+02	0.5677E−11	0.4513E+02
−0.2756E−10	0.2904E+02	0.3519E−11	0.2902E+02	−0.1802E−10	0.2914E+02	−0.6210E−11	0.2912E+02

R15-L.E.-T.E.; $\ell_{11} = 4, \ell_{22} = 4$
R16-L.E.-T.E.; $\ell_{11} = -4, \ell_{22} = 4$
R17-L.E.-T.E.; $\ell_{11} = 4, \ell_{22} = -4$
R18-L.E.-T.E.; $\ell_{11} = -4, \ell_{22} = -4$

TABLE 3. Variation With Single Control Mass Unbalance of
Complex Eigenvalues λ Using Complex Transfer Function

R50		R51		R52		R53	
λ_{Real}	$\lambda_{Imaginary}$	λ_{Real}	$\lambda_{Imaginary}$	λ_{Real}	$\lambda_{Imaginary}$	λ_{Real}	$\lambda_{Imaginary}$
0.1333E+00	0.3893E+03	−0.1318E+00	0.3893E+03	−0.6984E−01	0.3893E+03	0.7040E−01	0.3893E+03
0.1190E+01	0.3170E+03	−0.1188E+01	0.3166E+03	−0.6363E+00	0.3167E+03	0.6400E+00	0.3169E+03
0.3996E−01	0.2671E+03	−0.4062E−01	0.2671E+03	−0.3842E+00	0.2670E+03	0.3808E+00	0.2672E+03
−0.9477E−02	0.2277E+03	0.9560E−02	0.2277E+03	−0.1189E−01	0.2277E+03	0.1173E−01	0.2277E+03
0.2788E−02	0.1613E+03	−0.2789E−02	0.1613E+03	−0.8265E−02	0.1613E+03	0.8219E−02	0.1613E+03
−0.1761E−03	0.1203E+03	0.1741E−03	0.1203E+03	0.1721E−03	0.1203E+03	−0.1718E−03	0.1203E+03
0.1332E+00	0.9359E+02	−0.1313E+00	0.9343E+02	−0.2617E−01	0.9349E+02	0.2619E−01	0.9353E+02
0.4911E−01	0.8419E+02	−0.5072E−01	0.8413E+02	−0.1138E−01	0.8415E+02	0.1129E−01	0.8417E+02
0.2276E−02	0.4515E+02	−0.2266E−02	0.4515E+02	−0.9934E−02	0.4514E+02	0.9931E−02	0.4516E+02
0.1686E−01	0.2912E+02	−0.1678E−01	0.2904E+02	−0.2896E−02	0.2907E+02	0.2888E−02	0.2909E+02

R50-T.E. Only; $\ell_{22} = a(50)$
R51-T.E. Only; $\ell_{22} = -a(50)$
R52-L.E. Only; $\ell_{11} = a(50)$
R53-L.E. Only; $\ell_{11} = -a(50)$
$a(\omega)$ is defined in eq. (45)

TABLE 4. Variation With L.E.–T.E. Mass Unbalance of Complex Eigenvalues λ Using Complex Transfer Function

R54		R55		R56		R57	
λ_{Real}	$\lambda_{Imaginary}$	λ_{Real}	$\lambda_{Imaginary}$	λ_{Real}	$\lambda_{Imaginary}$	λ_{Real}	$\lambda_{Imaginary}$
-0.2010E+00	0.3893E+03	0.2042E+00	0.3893E+03	0.6289E-01	0.3893E+03	-0.6206E-01	0.3893E+03
-0.1828E+01	0.3165E+03	0.1827E+01	0.3171E+03	0.5563E+00	0.3169E+03	-0.5454E+00	0.3167E+03
-0.4229E+00	0.2670E+03	0.4226E+00	0.2672E+03	-0.3462E+00	0.2670E+03	0.3385E+00	0.2672E+03
-0.2363E-02	0.2277E+03	0.2213E-02	0.2277E+03	-0.2133E-01	0.2277E+03	0.2133E-01	0.2277E+03
-0.1102E-01	0.1613E+03	0.1104E-01	0.1613E+03	-0.5514E-02	0.1613E+03	0.5393E-02	0.1613E+03
0.3482E-03	0.1203E+03	-0.3460E-03	0.1203E+03	-0.5942E-05	0.1203E+03	0.3435E-06	0.1203E+03
-0.1568E+00	0.9342E+02	0.1601E+00	0.9360E+02	0.1064E+00	0.9357E+02	-0.1058E+00	0.9345E+02
-0.6237E-01	0.8412E+02	0.6014E-01	0.8420E+02	0.3798E-01	0.8419E+02	-0.3918E-01	0.8413E+02
-0.1222E-01	0.4513E+02	0.1219E-01	0.4517E+02	-0.7639E-02	0.4514E+02	0.7684E-02	0.4516E+02
-0.1964E-01	0.2903E+02	0.1978E-01	0.2913E+02	0.1393E-01	0.2911E+02	-0.1393E-01	0.2905E+02

R54—L.E.–T.E.; $\hat{\imath}_{11} = a(50), \hat{\imath}_{22} = -a(50)$
R55—L.E.–T.E.; $\hat{\imath}_{11} = -a(50), \hat{\imath}_{22} = a(50)$
R56—L.E.–T.E.; $\hat{\imath}_{11} = a(50), \hat{\imath}_{22} = a(50)$
R57—L.E.–T.E.; $\hat{\imath}_{11} = -a(50), \hat{\imath}_{22} = -a(50)$
$a(\omega)$ is defined in eq. (45)

NASA
National Aeronautics and
Space Administration

Report Documentation Page

1. Report No. NASA TP-2952	2. Government Accession No.	3. Recipient's Catalog No.
4. Title and Subtitle Effect of Control Surface Mass Unbalance on the Stability of a Closed-Loop Active Control System		5. Report Date October 1989
		6. Performing Organization Code
7. Author(s) E. Nissim		8. Performing Organization Report No. H-1534
		10. Work Unit No. RTOP 505-66-71
9. Performing Organization Name and Address NASA Ames Research Center Dryden Flight Research Facility P.O. Box 273, Edwards, CA 93523-5000		11. Contract or Grant No.
		13. Type of Report and Period Covered Technical Paper
12. Sponsoring Agency Name and Address National Aeronautics and Space Administration Washington, DC 20546		14. Sponsoring Agency Code

16. Abstract

The effects on stability of inertial forces arising from closed-loop activation of mass-unbalanced control surfaces are studied analytically using inertial energy approach, similar to the aerodynamic energy approach used for flutter suppression. The limitations of a single control surface like a leading-edge (L.E.) control or a trailing-edge (T.E.) control are demonstrated and compared to the superior combined L.E.–T.E. mass unbalanced system. It is shown that a spanwise section for sensor location can be determined which ensures minimum sensitivity to the mode shapes of the aircraft. It is shown that an L.E. control exhibits compatibility between inertial stabilization and aerodynamic stabilization, and that a T.E. control lacks such compatibility. The results of the present work should prove valuable, both for the purpose of flutter suppression using mass unbalanced control surfaces, or for the stabilization of structural modes of large space structures by means of inertial forces.

17. Key Words (Suggested by Author(s)) Active controls Aeroservoelasticity Control of space structures Flutter suppression		18. Distribution Statement Unclassified — Unlimited Subject category 39
19. Security Classif. (of this report) Unclassified	20. Security Classif. (of this page) Unclassified	21. No. of pages 25 22. Price A02